

# Design and Optimization of a Resonant Converter for Wireless Power Transfer

Nikolay Kalugin<sup>1</sup>, Valentin Gura<sup>1</sup>, Alexey Suvorin<sup>1</sup>, Andrey Kostin<sup>1</sup>

<sup>1</sup> EnerGET LLC, Russia

Nikolay Kalugin n.kalugin@energetpower.com

Nikolay Kalugin n.kalugin@energetpower.com

## Abstract

Electrified Transportation needs a source of electrical energy. One of possible power sources is a rechargeable battery. The vehicle's on-board battery is charged via power cable connected or by implementation of Wireless Power Transfer (WPT) technology. Basic WPT technology is strongly-coupled magnetic resonance. The resonance frequency and power transmitted is depending on the relative position of the transmitting and receiving windings. In this paper we consider resonance power converter for resonant WPT. Issues on power transmitted and resonant frequencies variations depending on the relative position of the transmitting and receiving coils are considered.

## 1 Introduction

Wireless power transfer is a technology to transmit power without wires. One or several transmitters generate an electromagnetic wave, which is processed by one or several receivers in order to extract power from the wave. Small power WPT charges are common for cellular phones charging. High power (up to 50 kW) WPT charging stations are used to charge electric cars. Unmanned aerial vehicle (UAV) are also the subject for WPT charge implementation. In this paper, we consider design and optimization of 500 W DC/DC for WPT prototype of charging station for small UAV. We also consider optimal configuration of compensating or resonate network and winding configurations.

## 2 Fundamentals of Wireless Power Transfer and optimization goals

### 2.1 Fundamentals of Wireless Power Transfer

Magnetic resonance, which is variant of inductive WPT [1], [2], [3] is used to charge vehicle. This means, that power converter operates at resonance frequency of a power transfer network. The network consists of compensating network, transmitting winding at primary side, receiving winding and compensating network at secondary side as it is shown in Fig. 1. Primary converter generates alternating voltage  $V_s$  at resonance frequency of transferring network, which consists of primary (transmitting)  $L_1$  and secondary (receiving)  $L_2$  windings with compensating networks and secondary side rectifier.

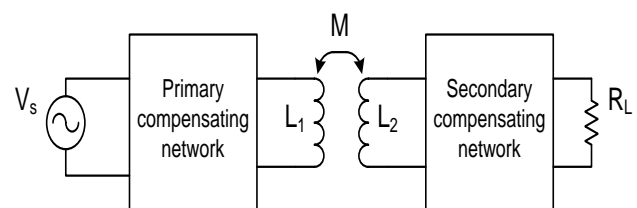


**Fig. 1.** Functional flow block diagram of the WPT system

The simple compensation network consists of a single capacitor, which may be connected to the primary and the secondary in series or in parallel. Alternative, more complex compensation topologies are also an option but they are not the subject of the paper. The geometry and materials of primary and secondary windings are crucial for determining the magnetic field of the WPT and its efficiency. Combinations of misalignments: vertical, horizontal and angular, affect the magnetic coupling and, consequently, the efficiency of energy transfer. Therefore, the compensating network configuration and winding geometry must be investigated to consider power transmission in case of misalignment.

### 2.2 Resonant network configuration

Single capacitor compensating network may be connected in series or in parallel to a winding of WPT systems, which provides four possible combinations of the resonance network (primary topology – secondary topology):

- Series – series;
- Series – parallel;
- Parallel – series;
- Parallel – parallel.

It is also necessary to mention, that secondary side winding (receiving) has the ability to operate without any compensating network and this option should also be studied. It is necessary to find the optimal combination of primary and secondary compensating networks. During calculations and simulations, misalignments are considered as a decrease in the magnetic coupling coefficient. The analysis of compensating networks was carried out in [1], [4], [5]. In [1] equations are derived to calculate expected efficiency of various compensating networks. Scheme for the series-series configuration is shown in Fig. 2.

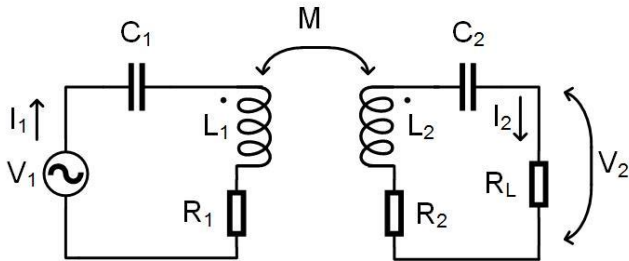


**Fig. 2.** Series-to-series configuration of compensating network

$V_1$  – alternating voltage source,  $R_1$  – equivalent series resistance (ESR) of primary winding  $L_1$ ,  $R_2$  – ESR of secondary winding  $L_2$ ,  $M$  – mutual inductance and  $R_L$  – load resistance. Consequently, efficiency is calculated as

$$\eta = \frac{R_L}{R_1 \left( \frac{R_2 + R_L}{\omega_0 M} \right)^2 + R_2 + R_1} \quad (1)$$

where

$$\omega_0 = \frac{1}{\sqrt{L_1 C_1}} = \frac{1}{\sqrt{L_2 C_2}} \quad (2)$$

is operational frequency. A parallel - parallel configuration of compensating network is shown in Fig. 3.

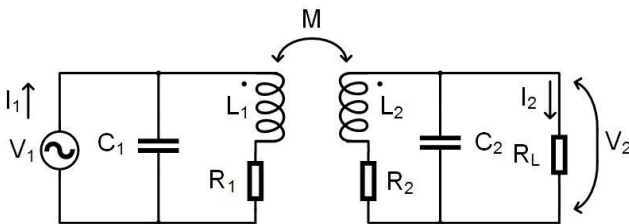


**Fig. 3.** Parallel-to-parallel configuration of compensating network

The efficiency for this case is proposed to be calculated as follows:

$$\eta = \frac{R_L}{\frac{R_1 L_2^2}{M^2} + R_2 + R_L} \quad (3)$$

Formulas (1)- (3) are derived based on a number of simplifications, most significant of which are that the resonance frequency does not depend on mutual inductance and that the load is a simple resistance. In practice resonance frequency depends on mutual inductance and the load is usually a battery and consumes

direct rather alternating current. Thus, additional simulation is required to find the optimal configuration of the compensating network.

## 2.3 Winding configuration and design

The optimal configuration of the windings depends on power transmitted and possible windings misalignments. The WPT charging station described has to take into account horizontal, vertical and angular misalignments. Therefore, we cannot use a pyramidal array [6] or a flat array [7] of transmission windings, so a two coil system will be applied and optimized as described in [8]. Thus, a configuration with flat transmitting and receiving windings was chosen.

## 3 Primary and secondary resonant network optimum design

### 3.1 SPICE model

In order to find the optimal configuration of the primary and secondary compensating network, schematic was assembled in LTSPICE. Primary side schematic is shown in Fig 4. NMOS transistors  $Q_1$ ,  $Q_2$  operates in auto-oscillating mode. Oscillating frequency is set by the resonant frequency of the transmitting winding  $L_{W1}$  and the compensating capacitor  $C_1$ . The values of the inductance  $L_{W1}$  and the resistance  $R_{S1}$  are obtained by measuring the assembled windings.

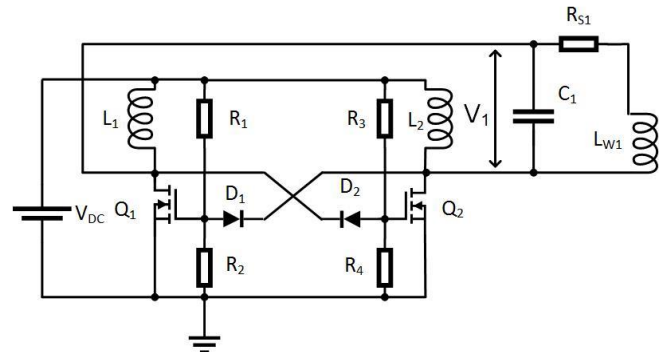


**Fig. 4.** Primary side simulating circuit, parallel compensation network

The primary side schematic with series compensating network is shown in Fig 5. Simulations was carried out both for the two previously mentioned circuits with a compensation capacitor on the secondary side and for the circuit without a compensating capacitor. During the simulation, the magnetic coupling was varied from 0.9 to 0.2. Voltage transferred from  $V_1$  to  $R_L$  was measured. Analysis of the simulation results shows that maximum power is transferred for combining a parallel capacitor connection on the primary side and uncompensated secondary side.

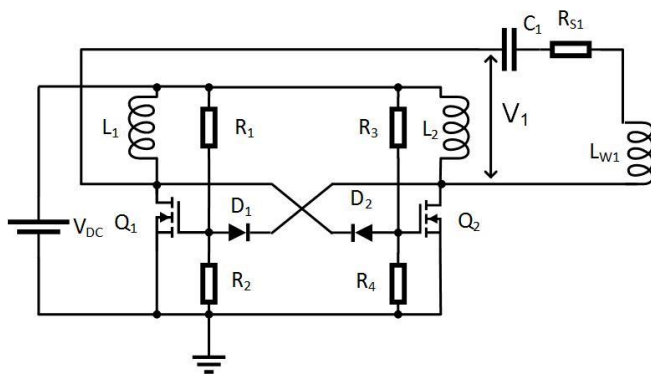


**Fig. 5.** Primary side simulating circuit, series compensation network

## 4 Determining the appropriate winding design

The receiving winding, in comparison with the transmitting one, may be:

- of equal diameter;
- of smaller diameter.

The decision should be made on the basis of the best energy transfer at various misalignments: vertical, horizontal and angular, as it is shown in Fig. 6.

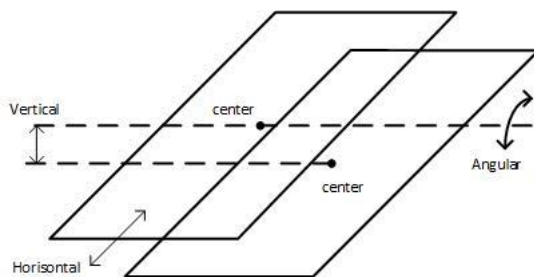


**Fig. 6.** Vertical, horizontal and angular misalignments

The influence of each misalignment must be investigated separately from the others. For this purpose, a testbench was assembled, that is shown in Fig. 7. The power circuit of the testbench corresponds to the circuit shown in Fig. 4. The transmitted power dependency on vertical, horizontal and angular position of the receiving winding was measured by the propose of the test bench.

The output voltage of the secondary side winding is rectified and then applied to a resistor, thus power transmitted is obtained by measuring DC voltage on the resistor.

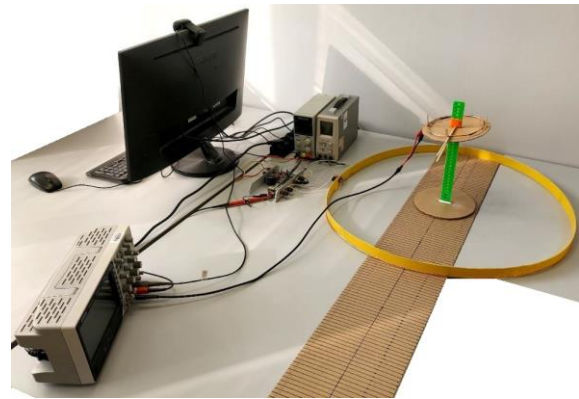


**Fig. 7.** Measuring the dependence of power transmission on three types of misalignments

At a fixed vertical distance, measurements were taken of the dependence of the transmitted power on the center-to-center distance of the two coils. At points with maximum transmitted power, measurements were carried out for varying the angle of inclination of the receiving winding and for varying the vertical distance. Two series of measurements were carried out: for windings of the equivalent diameter and for a receiving winding of a smaller diameter than the transmitting one. The graph of the dependence of the transmitted voltage on the center-to-center distance for small receiving winding is shown in Fig. 8.

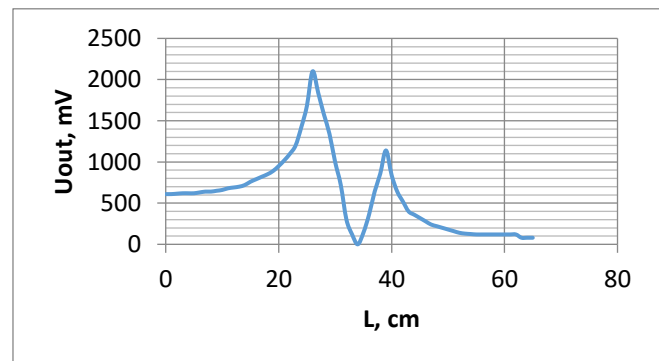


**Fig. 8.** Voltage transferred vs. center-to-center distance

The two distinct peaks in the graph correspond to edge positions inside and outside the transmitting winding. The minimum on the graph corresponds to the position when the center of the receiving winding is located strictly above the edge of the transmitting winding. The graph of the dependence of the transmitted voltage on the vertical distance is shown in Fig. 9 and Fig. 10. Fig. 9 shows the graph for aligned centers of transmitting and receiving windings. The graph of the dependence of the transmitted voltage on the vertical distance for first peak in Fig. 8 is shown in Fig. 10.

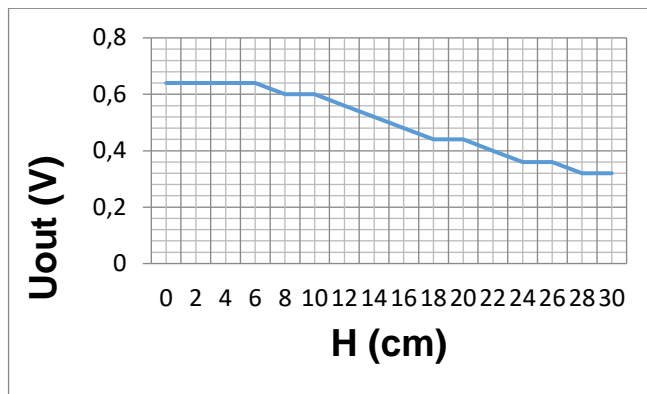


**Fig. 9.** Voltage transferred vs. vertical distance, centers are aligned

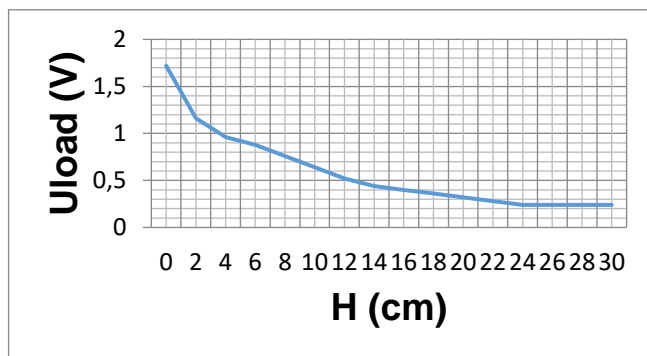


**Fig. 10.** Voltage transferred vs. vertical distance, at first peak point

Based on the measurements carried out, we conclude that the proper configuration is that with the diameter of the receiving winding significantly (3-5 times) smaller than the diameter of the transmitting winding.

## 5 Design on 500 W resonant converter

A 500 W resonant converter was designed with implementation of the results of previously described simulations and experiments. Input and output specifications of the converter are:

- Input voltage 380 – 420 V
- Output voltage 65 V
- Maximum output current 8 A
- Transmitting winding diameter 700 mm
- Transmitting winding inductance 35.2  $\mu\text{H}$
- Receiving winding diameter 150 mm
- Receiving winding inductance 2.3  $\mu\text{H}$

The input voltage of the converter is matched to the typical output voltage of a single phase PFC rectifier.

The primary side of the converter is the full bridge converter. The H-bridge is controlled by the FAN7631 IC. The IC is a resonant converter controller and its effectively adjusts the operating frequency to the resonant frequency of the combination receiving and transmitting winding. The secondary side is designed as full-wave rectifier with a center tap transformer and two NMOS

transistor as synchronous rectifiers. The generic diagram of the resonant converter is shown in Fig.11

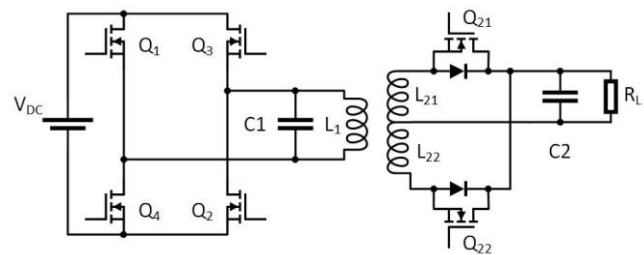


**Fig. 11.** Generic diagram of the resonant converter

A photo of the converter and the receiving and transmitting windings is shown in Fig. 12. It is shown in Fig 12 from left to right: the transmitting resonant converter, the receiving and transmitting coils, the receiving rectifier.

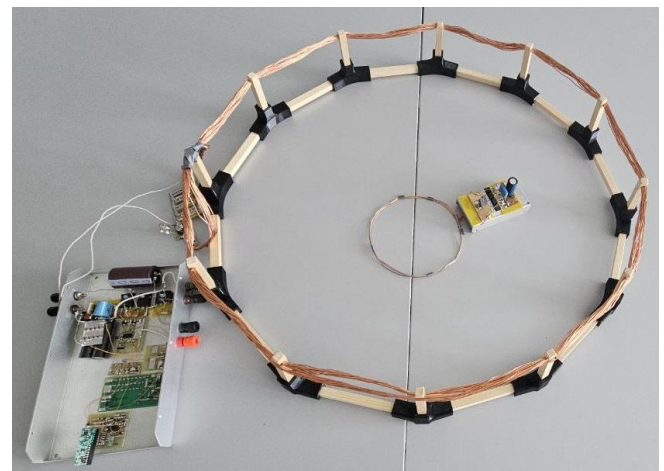


**Fig. 12.** The general view of wireless power transfer system

The dependence of the resonant frequency and efficiency on the distance between the windings is shown in Table 1.

**Table. 1.** Frequency and efficiency measurements results

Gap, mm	5	11	15	20	32	45	55	65
Reso- nant fre- quency, kHz	122	108	102	93	90	83	79	76
effi- ciency, %	92	92	92	91	88	85	80	75

## 6 Conclusions

Simulation and experiments on prototype shows that a parallel resonance converter on primary side is preferable for charging stations of small UAVs. The measurements also showed that it is necessary that receiving winding should be 3 to 5 times smaller in diameter than

the transmitting one. The solutions found were applied in a 500W converter layout and prototype tests confirmed the correctness of these conclusions. The operating frequency changes from 75 to 125 kHz and maximum efficiency of power transfer is 92 %.

## 7 References

- [1] Alicia Triviño-Cabrera , José M. González-González , José A. Aguado: *Wireless Power Transfer for Electric Vehicles: Foundations and Design Approach*. Springer Cham 2020 ISBN 978-3-030-26705-6
- [2] Kalwar, K.A., Aamir, M., Mekhilef, S.: Inductively coupled power transfer (ICPT) for electric vehicle charging A review. *Renew. Sustain. Energy Rev.* 47, 462–475 (2015)
- [3] Triviño-Cabrera, A., Aguado-Sánchez, J.: A review on the fundamentals and practical implementation details of strongly coupled magnetic resonant technology for wireless power transfer. *Energies* 11(10), 2844 (2018).
- [4] Jiang, Chaoqiang et al.: An Overview of Resonant Circuits for Wireless Power Transfer. *Energies* 10, 7 (June 2017): 894
- [5] Weijie Li, Lijun Diao, Weiyao Mei, Zhonghao Dongye, Xuqing Qin, Zheming Jin. Optimized Resonant Network Design for High Energy Transfer Efficiency of the WPT System April 2023 *Electronics* 12(9):1984
- [6] 750-W 85-kHz Inductive Rapid Charging System for Mid-sized UAV, Shuichi Obayashi, Yasuhiro Kanekiyo, Kiyokazu Sugaki, Akira Watabe, Hajime Nakakoji, Hiroshi Ichikawa, Noboru Takao, *Wireless Power Week Proceedings 2022 Bordeaux, France* 605 – 610
- [7] Mirbozorgi, S.A., Bahrami, H., Sawan, M., Gosselin, B.: A smart multicoil inductively coupled array for wireless power transmission. *IEEE Trans. Ind. Electron.* 61(11), 6061–6070 (2014)
- [8] J. P. K. Sampath, A. Alphones and D. M. Vilathgamuwa, "Coil optimization against misalignment for wireless power transfer,"2016 IEEE 2nd Annual Southern Power Electronics Conference (SPEC), Auckland, New Zealand, 2016, pp. 1-5, doi: 10.1109/SPEC.2016.7846159